SCIENTIFIC Publishing Limited

New Energy Exploitation and Application

https://ojs.ukscip.com/index.php/neea

Article

Advanced Thermal Management for PV Panels: Enhancing Efficiency with a Three-Dimensional Pulsating Heat Pipe

Mahyar Kargaran [1,*], Hamid Reza Goshayeshi [1] and Pooya Goshayeshi [2]

[1] Department of Mechanical Engineering, Mashhad Branch, Islamic Azad University, Mashhad 9187147578, Iran

[2] Department of Computer Engineering, Mashhad Branch, Islamic Azad University, Mashhad 9187147578, Iran

[*] Correspondence: m.kargaran@gmail.com

Received: 9 July 2025; **Revised:** 29 July 2025; **Accepted:** 12 August 2025; **Published:** 26 August 2025

Abstract: Harnessing solar energy represents a fundamental pillar of the global transition toward sustainable energy systems due to its abundance, renewability, and broad accessibility. Photovoltaic (PV) technology, in particular, has emerged as the most extensively deployed solution across residential, commercial, and utility-scale applications. However, the relatively low energy conversion efficiency of PV modules remains a critical challenge, with elevated operating temperatures being one of the primary factors contributing to performance degradation. Excessive heat not only reduces instantaneous electrical output but also accelerates material aging, thereby shortening the service life of PV systems. Consequently, the development of efficient cooling strategies has attracted considerable research attention. In this study, an advanced passive thermal regulation approach based on three-dimensional pulsating heat pipes (PHPs) was experimentally investigated. Two different inner diameters (2 mm and 3 mm) were designed, and their performance was evaluated using deionized water and graphene oxide (GO) nanofluid as working fluids. The results demonstrate that PHP integration can effectively reduce PV module surface temperatures, leading to notable improvements in electrical efficiency. The most significant enhancement was observed with GO nanofluid at a concentration of 0.8 g/L in 2 mm inner diameter PHPs, achieving up to a 3.2% increase in daily power generation compared with the baseline. Conversely, increasing the pipe diameter reduced the cooling effectiveness, underscoring the importance of geometric optimization and working-fluid selection in the design of PHP-assisted PV cooling systems.

Keywords: Solar Panel; Pulsating Heat Pipe; Nanofluid; Energy Efficiency; Thermal Management

1. Introduction

Renewable energy, especially solar energy, has drawn much attention in terms of power generation since there is a dire need to reduce greenhouse gases such as carbon dioxide [1]. Solar energy is the most integrated source of renewable energy. On the other hand, electricity is an inseparable energy need in all countries. Photovoltaic panels (PV panels), commonly referred to as solar panels, are devices used to transform energy from sunlight into electricity. PV panels have become increasingly popular as a renewable energy source due to their ability to generate electricity without producing greenhouse gas emissions or other pollutants [2]. They are used in a variety of applications, from residential installations to solar farms. As technology advances and costs decrease, solar panels are becoming more efficient and affordable, making solar irradiation a valuable choice for addressing climate change and reducing dependence on fossil fuels [3].

PV efficiency is typically defined as the portion of sunlight that is converted into electrical energy. The effi-

ciency of solar panels depends on various factors, including material, design (cell size, arrangement, and wiring configuration), and environmental factors (temperature, light spectrum, shading, dirt, and dust) [4]. Solar panel efficiency tends to decrease as temperature increases. High temperatures can reduce the efficiency of solar cells, so panel placement and cooling mechanisms can influence overall efficiency [5]. Over the years, there have been significant advancements in photovoltaic technology, leading to improvements in efficiency. Early solar panels had efficiencies of around 10–15%, while modern commercial panels typically range from 15–22% efficiency [6]. Development efforts continue to focus on enhancing efficiency and reducing costs to make solar energy even more competitive with conventional energy sources. Major cooling techniques used to reduce the operating temperature of solar panels to enhance their efficiency and prolong their lifespan are listed in **Figure 1**.

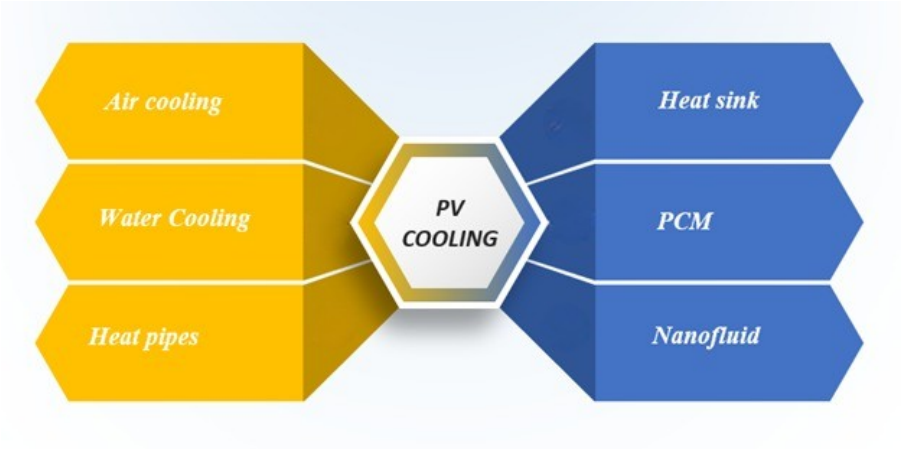

Figure 1. Cooling approaches of solar panels [7–12].

The selection of an appropriate cooling strategy for photovoltaic (PV) systems is influenced by several factors, including climatic conditions, system architecture, economic constraints, and the specific operational requirements of the solar installation. Effective thermal management plays a critical role in enhancing the electrical output and extending the service life of PV panels, thereby improving the overall system efficiency and economic viability. However, conventional cooling approaches—such as air and water cooling—are often limited by inherent drawbacks, including low thermal efficiency and susceptibility to freezing in cold environments. Heat pipes are considered a great solution to address these problems, significantly contributing to improved photovoltaic efficiency. There is a wide range of heat pipes (thermosyphons, loop heat pipes, rotating heat pipes, cryogenic heat pipes, variable conductance heat pipes (VCHPs), and pulsating heat pipes), which offer high performance in terms of heat transfer. Heat pipes are highly advantageous due to their low weight, cost-efficiency, reliability, and easy-to-manufacture structure [13]. The efficiency of pulsating heat pipes, also known as oscillating heat pipes, is a critical aspect of their performance and determines their suitability for various thermal management applications. The efficiency of a PHP can be evaluated based on several key performance metrics, including thermal resistance and heat transfer coefficient. Major factors influencing PHP efficiency are the heat source [14], filling ratio, number of twists [15], the inner diameter of the tubes [16], inclination angle [17], and the length of tubes [18], for example.

The emergence of the pulsating heat pipe (PHP) in the early 1990s [19] as one of the most efficient, innovative pieces of equipment has drawn much attention, thanks to its impressive performance in terms of heat transfer and unique design.Since PHPs are a type of heat pipe that relies on the oscillatory motion of the coolant within a capillary tube to transfer heat, the diameter of the tubes in a PHP significantly influences its thermal performance and thermal resistance. Too small or too large diameters can increase thermal resistance due to ineffective fluid motion or inadequate capillary action. On the other hand, a proper diameter promotes efficient capillary action and oscillatory fluid motion, decreasing thermal resistance. Lin et al. [20] experimented on heat pipes with two different diameters, namely 4 and 3 mm, and found that the larger diameter offered better performance. Rittidech et al. [21] inspected the thermal efficiency of a solar collector in conjunction with PHP and considered R134a as a working fluid. According to the study, the system successfully addressed the freezing problem and provided an

efficiency greater than 60%. Kargarsharifabad et al. [22] performed a study on the effect of geometric design and operating conditions on the performance of a PHP attached to a PVT. The system experienced maximum efficiency around 61% when the filling ratio was over 56%. In a comprehensive experimental study, Patel et al. [23] investigated the performance of eleven different working fluids in a pulsating heat pipe (PHP) integrated with a solar water heating system. The tested fluids included pure substances such as deionized (DI) water, acetone, methanol, and ethanol, along with binary mixtures formed by combining water with each of these pure fluids. Among the pure fluids, acetone exhibited the highest thermal performance, while the water–acetone mixture emerged as the most effective binary fluid. In another study, Roslan and Hassim [24] applied PHP technology for thermal management of photovoltaic panels, achieving a peak electrical efficiency slightly exceeding 19%. The introduction of nanofluids—engineered colloidal suspensions composed of nanoparticles dispersed in a base fluid—has further expanded the potential of thermal control systems by enhancing heat transfer characteristics [25]. Evidence indicates that adding nanoparticles significantly improves the thermal conductivity of the coolant, leading to more efficient heat transfer [26]. Shafiey et al. [27] investigated the efficiency of a heat pipe solar panel applying Al_2O_3, MgO, and CuO nanofluids. They found that the nanofluids improved the panel efficiency by more than 9% compared to water. Allouhi et al. [28] conducted numerical investigations on cooling solar collectors with HP for three different nanofluids (CuO, Al_2O_3, and TiO_2) and found that the system with CuO-based nanofluid could improve the system efficiency by around 11.1%.

Graphene oxide (GO)-based nanofluids have emerged as promising candidates for enhancing the thermal performance of heat pipes due to their superior thermal conductivity and efficient heat transfer characteristics [29]. Their favorable dispersion stability within base fluids plays a critical role in ensuring consistent and reliable thermal behavior during operation [30]. Although both two-dimensional and three-dimensional pulsating heat pipes (PHPs) are effective for thermal regulation, 3D PHPs offer distinct advantages in high-power and multi-directional thermal applications owing to their improved heat transfer capacity and complex internal flow dynamics [31,32]. In a study conducted by Thompson et al. [33], three-dimensional flat-plate oscillating heat pipes (3D FP-OHPs) charged with either water or acetone were tested, with water achieving the lowest thermal resistance of 0.08 °C/W. Similarly, Ling et al. [34] demonstrated that integrating a phase change material (PCM) with a 3D PHP cooling system in electronic devices resulted in up to a 36.3% reduction in thermal resistance, effectively enhancing heat dissipation to the surrounding environment. Qu et al. [35] conducted an experimental investigation into the thermal improvement of a composite phase change material (PCM) made of expanded graphite and octadecanol using 3D-PHP. Their findings revealed that the 3D-OHP reduced the charging time by 32% compared to traditional heat pipes. Pagliarini et al. [36] observed that a 3D-configuration pulsating heat pipe (PHP) maintained gravity-independent performance even under high heat loads.

Jung et al. [37] conducted a comparative analysis between a three-dimensional pulsating heat pipe (3D-PHP) and a conventional PHP, revealing that the 3D configuration exhibited enhanced heat transfer performance. This improvement was attributed to the presence of additional flow pathways, which led to a reduction in thermal resistance by up to 14.7% and a decrease in evaporator temperature by 6.7 °C under uniform heating conditions. In a separate study, Dia et al. [38] developed an innovative 3D-PHP design and systematically evaluated the influence of geometric parameters and operating conditions on its thermal performance. Their findings highlighted that a more uniform distribution of vapor-liquid plugs significantly contributes to the efficient operation of the PHP, emphasizing the importance of flow stability in maximizing heat transfer effectiveness.

Despite these advancements, two critical gaps remain in the current literature:

Scarcity of studies on three-dimensional pulsating heat pipes (3D-PHPs), which offer superior heat transfer capability and multi-directional heat management suitable for high-power applications. While some numerical and experimental studies on 3D-PHPs exist, most do not focus on PV integration.

Lack of experimental data on the effect of inner diameter of the heat pipe in 3D configurations, particularly considering the influence of dimensionless parameters like the Eötvös number, which governs capillary and gravitational forces in multiphase flow.

To address these gaps, this study introduces a novel 3D-PHP cooling system integrated with a PV panel, using deionized (DI) water and graphene oxide nanofluid as working fluids. The primary aim is to experimentally investigate the impact of inner diameter on thermal and electrical efficiency of the PV system. The study is unique in evaluating the combined effect of geometry, nanofluid enhancement, and passive operation, thereby offering a

self-sustaining and cost-effective solution for solar panel cooling.

By tackling a specific and previously underexplored parameter—the inner diameter of 3D-PHPs in solar applications—this research not only fills a significant knowledge gap but also proposes a practical and energy-efficient cooling strategy for real-world PV systems.

2. Setup Procedure

2.1. Experiment Setup

The experimental study was conducted in Mashhad, Iran, utilizing two monocrystalline photovoltaic (PV) panels—one equipped with a cooling system and the other serving as a reference unit without cooling. The electrical characteristics of the PV modules are presented in **Figure 2**.

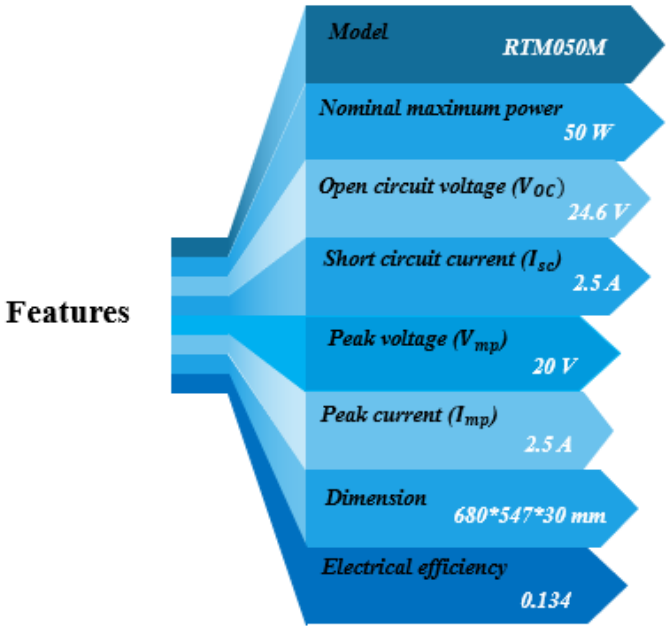

Figure 2. Electrical characteristics of the photovoltaic module.

Figure 3 depicts the new 3D-PHP made with copper. **Table 1** demonstrates the geometric parameters of the 3D-PHP. In this study, two PHPs with different diameters and a thickness of 1 mm were also used.

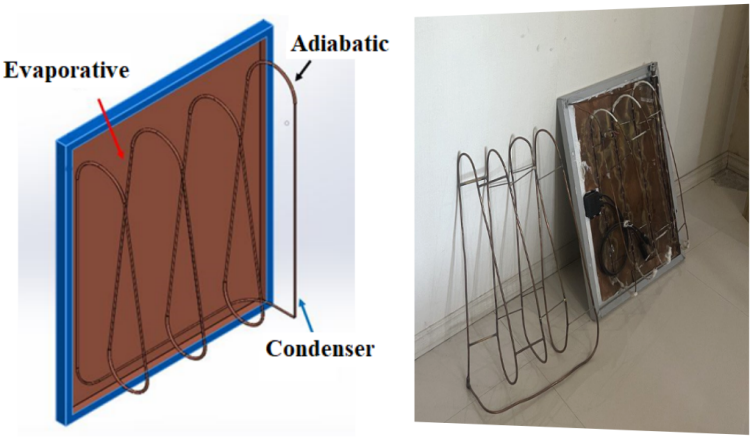

Figure 3. Structural layout of the PHP.

Table 1. Design parameters of PHP.

Parameters	Value
Number of turns	4
Evaporator	200 cm
Condenser	200 cm
Adiabatic	109 cm
Inner diameter	3.2
Outer diameter	5.4

It has been proven that PHP delivers optimum performance at a 50% filling ratio [39,40]; therefore, all the tests were conducted at 50%. The experimental setup is shown in **Figure 4**, while a schematic of the experiment is depicted in **Figure 5**.

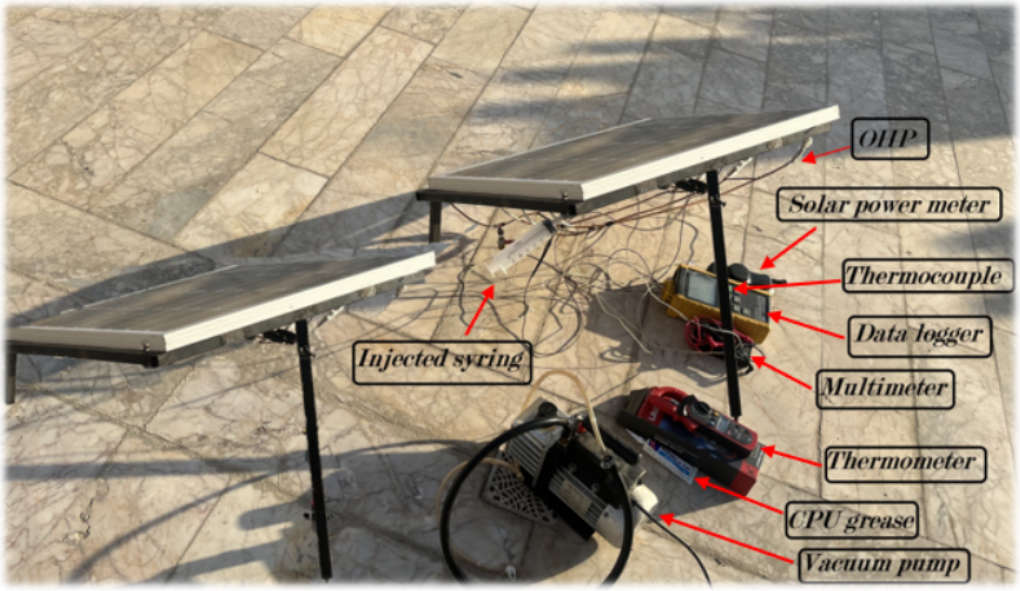

Figure 4. Experiment bed [2].

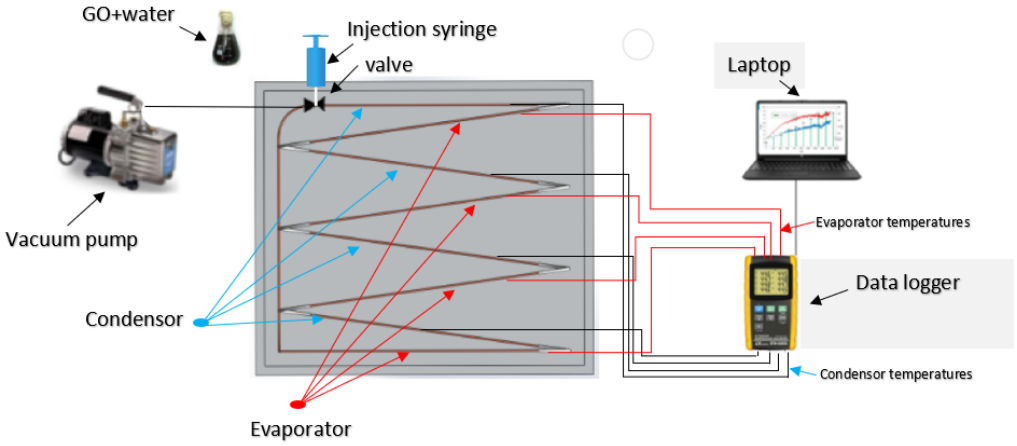

Figure 5. Schematic diagram of the experiment [2].

Although numerous studies have employed lamination techniques to secure the evaporator onto solar panels [41], this investigation utilized a copper sheet affixed to the panel surface with thermal paste, thereby reducing

operational costs and streamlining the assembly process. The cooling medium consisted of a graphene oxide (GO) nanofluid prepared at a concentration of 0.8 g/L, using distilled water as the base fluid. The GO nanoparticles were sourced from US Research Nanomaterials, Inc. Nanofluids are known to improve the thermal conductivity of base fluids; however, maintaining their dispersion stability is critical for sustained performance [42]. To enhance stability, the surfactant sodium dodecyl sulfate was incorporated into the nanofluid formulation. A scanning electron microscopy (SEM) image of the GO nanoparticles is presented in **Figure 6**.

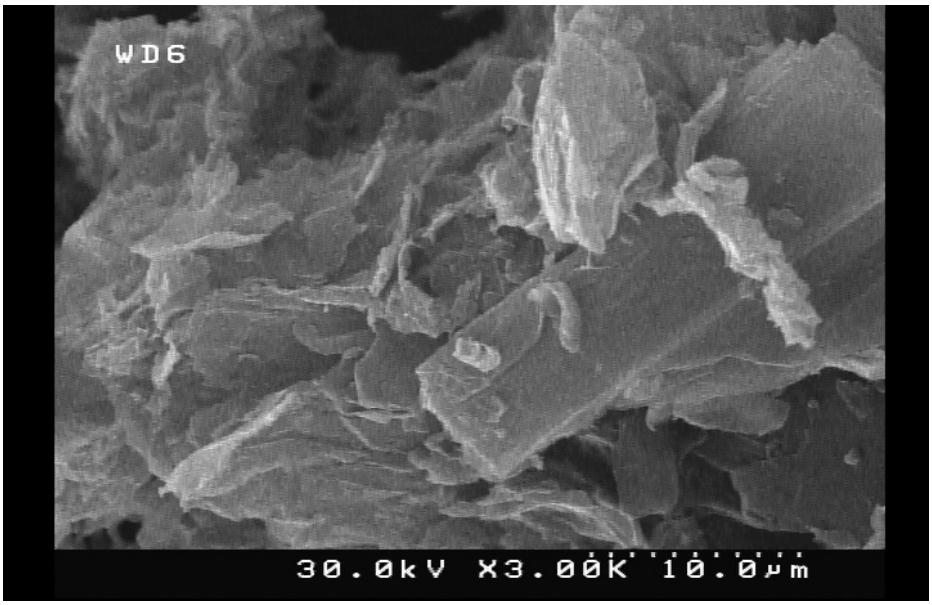

Figure 6. SEM of GO [2].

Figure 7 presents the Raman spectroscopy results of graphene oxide (GO), highlighting its distinctive characteristic peaks, notably near 1,400 cm^{-1} for the D band and 1,600 cm^{-1} for the G band of graphene oxide.

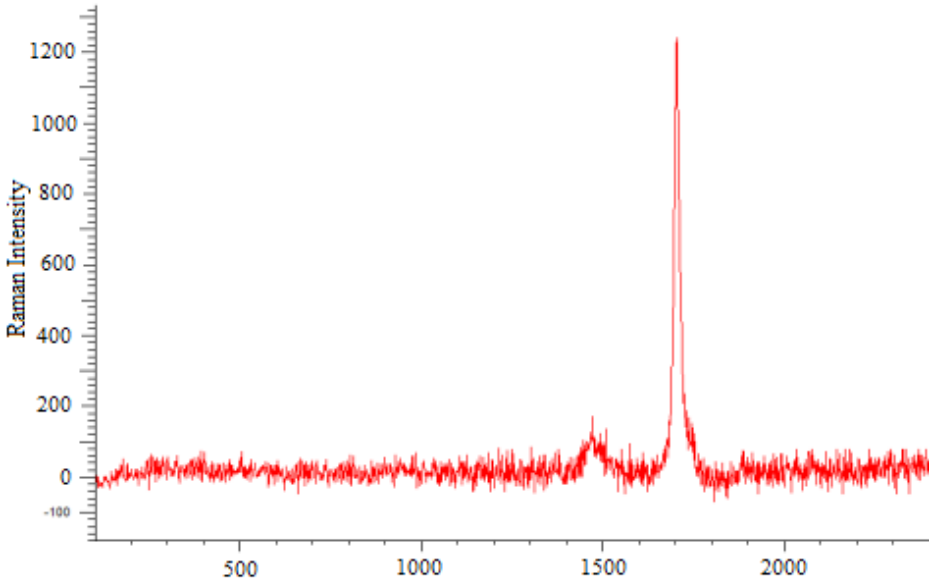

Figure 7. Raman spectroscopy analysis of GO.

Table 2 summarizes the measured thermal conductivity values of both the GO nanofluid and deionized (DI) water employed in this study.

Table 2. Thermal conductivity of coolant.

Coolant	Thermal Conductivity (W/K.m)
DI water	0.614
0.8 gr/lit	0.656

Future studies should incorporate a more diverse range of testing conditions to assess the system's adaptability. This includes varying the panel inclination angle, testing under different solar radiation profiles (seasonal variation), and evaluating multiple nanofluid concentrations to establish optimal formulations. Additionally, real-time energy consumption analysis and long-term durability testing are essential for practical deployment.

2.2. Data Processing

This section illustrates the analyses of heat transfer and energy conversion for the proposed system. The solar irradiation absorbed by the PV panel is expressed as Equation (1) [43]:

$$Q_a = \alpha_{PV}\beta_{PV}AG \tag{1}$$

A portion of the absorbed energy is converted into electricity, which can be determined by using Equation (2):

$$Q_{el} = \eta_{el}AG \tag{2}$$

And η_{el} represents the electrical efficiency, which is derived from Equation (3) [43].

$$\eta_{el} = \eta_{rc}\left[1 - \beta_{PV}\left(t_{PV} - t_{rc}\right)\right] \tag{3}$$

Where t_{rc} is reference temperature (25 °C). Heat loss from the panels to the surroundings is calculated using Equation (4) [43]:

$$Q_{loss} = \left(t_{PV} - t_{rc}\right) 0.664 \frac{\gamma_{air}}{L_{PV}} \mathrm{Re}_{air}{}^{1/2} Pr_{air}{}^{1/3} \tag{4}$$

In this study, Q_{loss} is considered negligible because the copper sheet on the back of the solar panel enhances heat exchange and functions as the evaporator for the PHP, thereby reducing heat loss. As a result, the remaining energy is transferred to the PHP (Equation (5)).

$$Q_{PHP} = Q_a - Q_{el} \tag{5}$$

For temperature measurement, eight K-type thermocouples were strategically positioned, with four sensors installed in the condenser section and another four in the evaporator section. The recorded temperature data were then processed using the following Equations (6) and (7):

$$T_e = \frac{T_{e1} + T_{e2} + T_{e3} + T_{e4}}{4} \tag{6}$$

$$T_c = \frac{T_{c1} + T_{c2} + T_{c3} + T_{c4}}{4} \tag{7}$$

The thermal resistance is given as Equation (8) [43]:

$$R = \frac{\Delta T}{Q_{PHP}} \tag{8}$$

And ΔT is calculated using Equation (9):

$$\Delta T = T_e - T_c \tag{9}$$

Therefore, the electrical efficiency of the solar panel—representing the fraction of incident solar radiation converted into electrical power—is determined using Equation (10) [44].

$$\eta_{el} = \frac{P_{out}}{P_{in}} = \frac{V_{mp} I_{mp}}{AG} \tag{10}$$

The efficiency enhancement achieved by the proposed system is quantified using Equation (11):

$$\eta_{im} = \frac{\eta_{PHP-PV}}{\eta_{PV}} - 1 \tag{11}$$

The Eötvös number (also known as the Bond number, Bo) is a dimensionless number that characterizes the relative importance of gravitational forces compared to surface tension forces acting on a fluid. It is particularly relevant in the context of heat pipes and nanofluids, as it helps in understanding the fluid behavior under the influence of gravity and surface tension. For a graphene oxide nanofluid in a heat pipe, the Eötvös number can provide insights into the performance and effectiveness of the nanofluid in terms of heat transfer and fluid dynamics. It is defined as Equation (12):

$$E_O = \frac{\Delta \rho g D_i^2}{\sigma} \tag{12}$$

Adding graphene oxide nanoparticles to DI water produces a negligible impact on its surface tension [45]. Nanoparticles can influence surface tension and decreases with increasing temperature. For graphene oxide nanofluids with a 0.8 g/L concentration, the surface tension varies between 0.0759 N/m at 20 °C and 0.0706 N/m at 60 °C.

The density of the nanofluid can be approximated using the weighted average of the densities of the base fluid and the nanoparticles Equation (13):

$$\rho_{nf} = (1 - \phi)\rho_{water} + \phi \rho_{GO} \tag{13}$$

The value for GO nonfluid varies from 998.6 kg/m^3 at 20°C to 983.6 kg/m^3 at 60°C. Density difference is also derived from Equation (14):

$$\Delta \rho = \rho_{nf} - \rho_v \tag{14}$$

Given that graphene oxide nanoparticles remain in the liquid phase, the presence of graphene oxide at 0.8 gr/lit concentration does not affect the vapor density of water (ρ_v). Therefore, the vapor phase density can be assumed to be the same as that of pure water vapor. Vapor phase density of water at 60 °C and 20 °C is approximately 1.663 kg/m^3 and 0.0173 kg/m^3, respectively. Adding surfactant sodium dodecyl sulfate, which lowers the surface tension, significantly contributes to optimizing the Eötvös number, bringing it into the optimal range (1 to 5) for pulsating heat pipes [46], which suggests improved conditions for the oscillatory motion of the working fluid, leading to potentially better performance of the heat pipe. The value for GO when D_i = 2 mm is $E_O \approx 1.14$ and $E_O \approx 1.31$, for 20 °C and 60 °C, respectively. While in the absence of sodium dodecyl sulfate, the Eötvös number for temperatures ranging from 20 °C to 60 °C is less than 1.

2.3. Uncertainties

Ensuring the accuracy of experimental data is critical in this study. Consequently, an uncertainty analysis was performed to assess the reliability of the measured results. The uncertainties were evaluated considering both direct measurements and derived calculations, following the methodology outlined in thw work of Santbergen et al. [47]. Measurement instrument errors and data acquisition inaccuracies were quantified and are summarized in **Table 3**.

Table 3. Uncertainty of values.

Value	Uncertainty
T_a (°C)	± 0.1
T_c (°C)	± 0.1
T_e (°C)	± 0.1

Table 3. *Cont.*

Value	Uncertainty
T_s (°C)	± 0.1
G (W/m²)	± 1.0
S_w (m/s)	± 0.1
V_{OC} (V)	± 0.04
I_{sc} (A)	± 0.0014

3. Results and Discussion

The temperature, power, and efficiency of the solar panels have been calculated. A series of tests was conducted on days when the sky was clear. The tests were performed under the climatic conditions of Mashhad, Iran. Furthermore, two panels were used: one equipped with a 3D-PHP and the other serving as a reference collector.

3.1. Initial Conditions

As shown in **Figure 8**, the ambient temperature, and consequently the solar collector temperature, increases until it peaks at mid-day. Afterward, both temperatures decrease. Similarly, solar intensity exhibits a similar pattern, reaching over 1120 W/m^2 at 11:30, while the minimum value recorded is 750 W/m^2 (**Figure 9**).

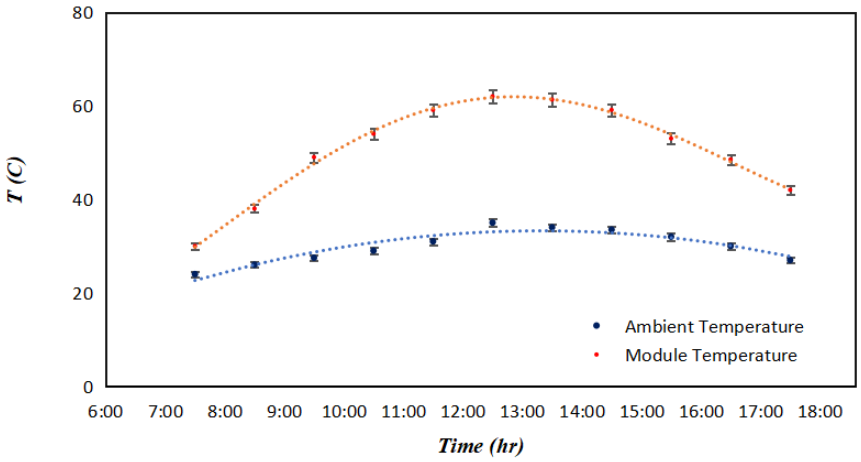

Figure 8. The variations in ambient temperature alongside the solar panel temperature.

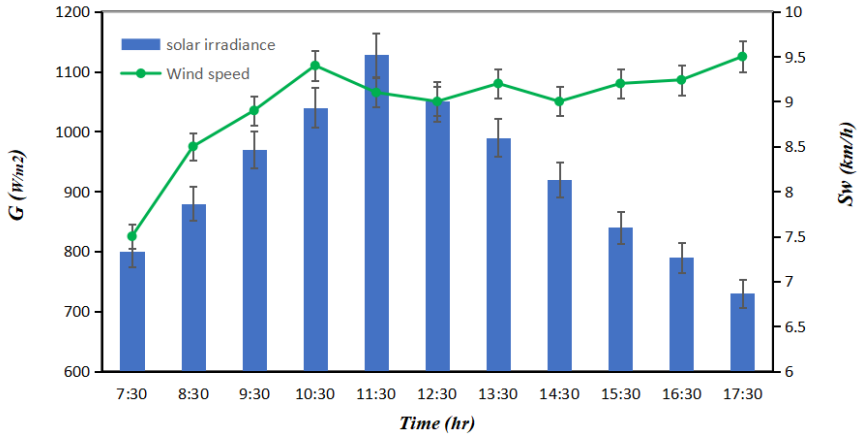

Figure 9. Solar irradiance and wind speed.

Wind speed is a significant factor impacting both the efficiency of the solar panel and the performance of the pulsating heat pipe (PHP). As shown in **Figure 9**, the average wind speed gradually increases throughout the testing period, exceeding 9 km/h by the conclusion of the experiment. The electrical efficiency of the PV panel is primarily governed by solar irradiance and panel temperature [48]. Generally, higher solar irradiance corresponds to improved efficiency; however, the short-circuit current (I_{sc}) and open-circuit voltage (V_{OC}) respond inversely to changes in panel temperature, as depicted in **Figure 10**.

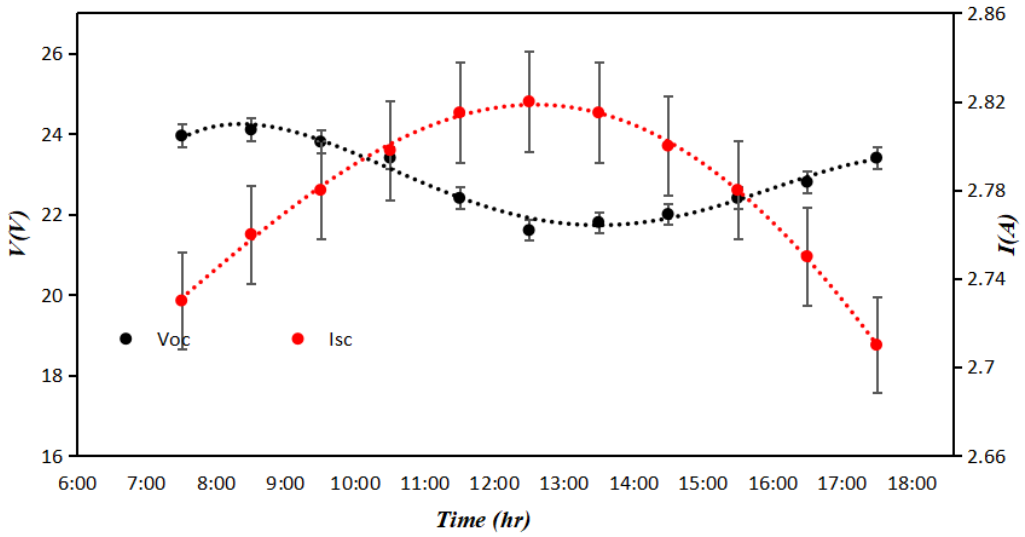

Figure 10. I_{sc} and V_{OC} behavior during the test.

3.2. System Performance

Solar panels are responsible for capturing sunlight and converting it into electricity. The larger the area covered by solar panels, the greater the chance of capturing the sun's energy. One parameter that strongly influences the efficiency of a solar panel is its angle of tilt relative to the horizon, which affects the amount of solar radiation received. Therefore, panels need to be tilted at the optimal angle to achieve maximum efficiency [49].

In this study, the system was tested at a 30° tilt angle, which is considered the optimal angle for solar collectors in Mashhad according to Kargaran et al. [50]. **Figure 11** demonstrates the start-up time for different coolants and tube diameters during the test day. It was found that the diameter significantly affects the start-up time of the PHP. When D_i = 3 mm, the heat pipe starts to operate after 80 to 100 minutes with GO and DI water as coolants, while the start-up time decreases considerably when D_i = 2 mm.

The start-up behavior of the pulsating heat pipe was strongly influenced by both the inner diameter and the type of coolant used. **Figure 11** illustrates the evolution of surface temperatures for the PV panel and the PHP during the initial heating phase.

The PHPs with a 2 mm inner diameter demonstrated faster thermal activation compared to those with a 3 mm diameter. Specifically, using deionized water or graphene oxide (GO) nanofluid, the 2 mm systems initiated pulsating activity between 55.6 °C and 56.9 °C, which corresponded to PV surface temperatures of ~ 60.5–61.5 °C. In contrast, the 3 mm diameter PHPs required longer heating durations, with start-up occurring only after the panel reached higher temperatures, typically above 57.5 °C, translating to 80–100 minutes under full solar load.

This difference is attributed to the increased capillary action and vapor pressure gradient within narrower tubes. According to PHP theory, a reduced diameter enhances the interaction between vapor plugs and liquid slugs, promoting more vigorous oscillations at lower wall superheats. This effect is particularly critical in horizontal or low-inclination orientations, where gravity-driven return flow is minimized.

Furthermore, the inclusion of graphene oxide nanofluid improved start-up conditions across both diameters. For 2 mm PHPs, the GO coolant consistently yielded surface temperatures 1.5–2.5 °C lower than water, suggesting more efficient early-phase heat transfer. The improvement is likely due to the enhanced thermal conductivity and

reduced surface tension of GO nanofluids, which contribute to better nucleation and more stable oscillations.

These findings are aligned with earlier studies [4,5] and emphasize the importance of geometric-fluid matching in optimizing PHP start-up dynamics for solar thermal regulation.

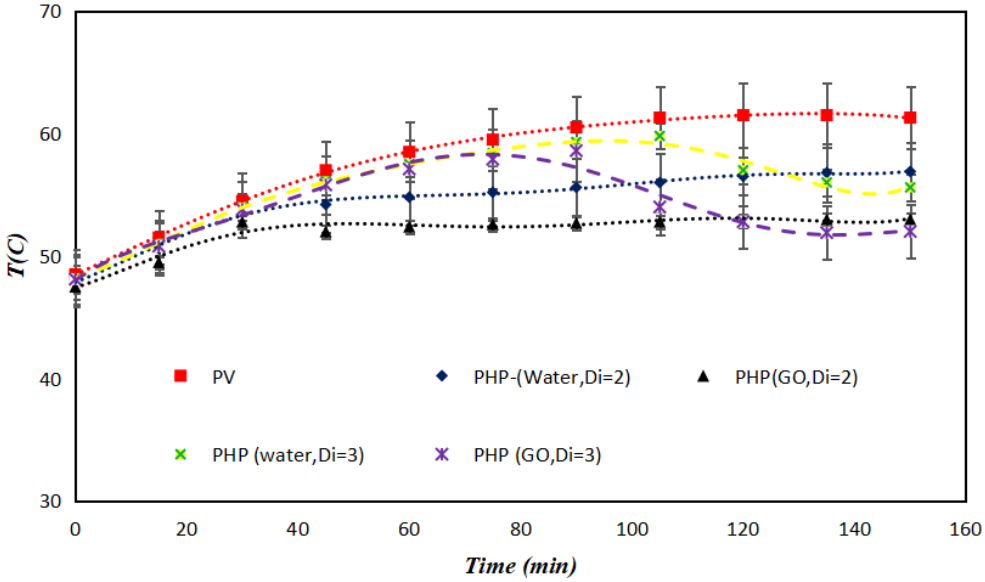

Figure 11. Effect of coolant and diameter on start-up time.

As illustrated in **Figure 12**, the thermal resistance of the 3D pulsating heat pipe (3D-PHP) is highly dependent on both the working fluid and the internal diameter of the pipe. In all tested configurations, thermal resistance exhibited a declining trend with increasing heat input, reflecting enhanced phase-change dynamics and more vigorous oscillatory flow within the PHP. The configuration using graphene oxide (GO) nanofluid with a 2 mm inner diameter achieved the lowest thermal resistance value of 0.78 K/W, outperforming the corresponding 3 mm GO case (0.80 K/W) and all water-based configurations. This improvement can be attributed to the superior thermal conductivity and surface activity of GO nanofluid, which promotes rapid vapor bubble generation and accelerates fluid motion through the capillary channels.

Water-based systems, by comparison, consistently exhibited higher thermal resistance, particularly in the 3 mm diameter setup, where diminished capillary dominance delayed the onset of oscillations and reduced thermal transport efficiency. The data emphasize that reduced internal diameter strengthens capillary action, facilitating frequent vapor-slug formation and more effective heat transfer along the evaporator–condenser pathway [4]. Although larger diameters increase available flow volume, they hinder capillary-induced motion, especially under low-to-moderate heat flux, resulting in slower thermal response and elevated resistance.

Nevertheless, the introduction of GO nanofluid helps counterbalance these geometric limitations by enhancing thermal performance even in less favorable tube dimensions. These results highlight the importance of simultaneously optimizing working fluid characteristics and geometric design to achieve minimal thermal resistance. The findings reinforce the potential of GO-enhanced, small-diameter PHPs as a robust and passive cooling solution for photovoltaic thermal applications, particularly where compactness, energy independence, and operational reliability are essential.

As the diameter increases beyond a critical value, the dominance of capillary forces decreases, which can impair the efficiency of capillary action. This leads to less effective fluid oscillations and higher thermal resistance. The maximum performance of the solar panel occurs at 25 °C; temperatures above this result in performance loss due to high temperatures, which strongly affects performance. In this experiment, maximum P_{out} suffers a major loss especially at midday. At the beginning, PHP with D_i= 2 showed better performance, but over time, PHP with D_i= 3, offers higher performance especially when graphene oxide was employed as a coolant (**Figure 13**).

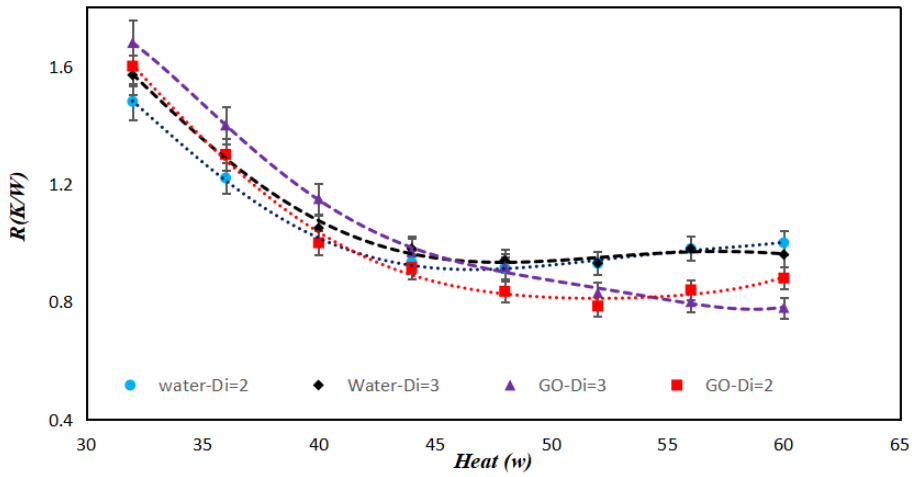

Figure 12. Thermal resistance vs received heat.

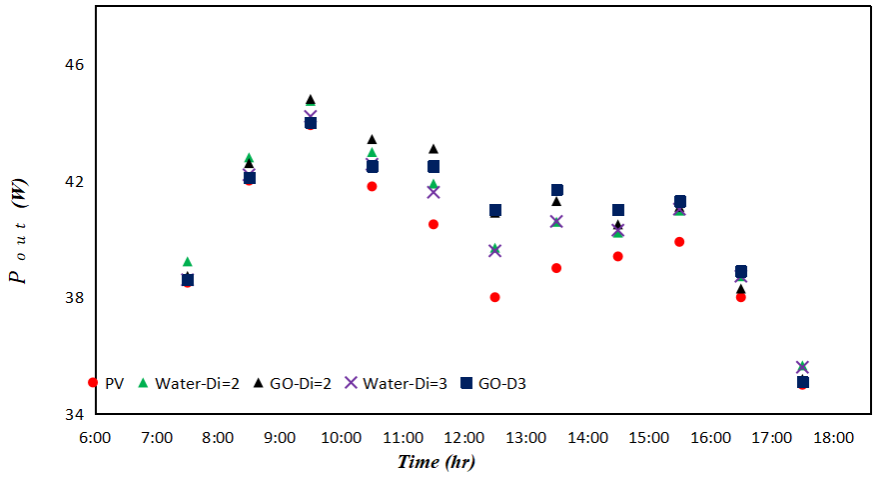

Figure 13. Effect of coolants and diameter on P_{out}.

As shown in **Figure 14**, the electrical efficiency of the PV panels is inversely related to surface temperature. During the test day, as solar irradiance increased and temperatures peaked around midday, all systems experienced a decline in PV efficiency. This trend is consistent with the well-established temperature sensitivity of photovoltaic cells, where rising cell temperature reduces open-circuit voltage, thereby lowering power output. However, the PHP-integrated systems—especially those employing GO nanofluid—effectively mitigated this loss through enhanced cooling performance. Among all configurations, the 2 mm GO-based PHP consistently delivered the highest PV efficiency, reaching a peak of 0.1318, compared to 0.1297 for the best-performing 3 mm GO case, and 0.1289 for the 2 mm water-cooled system.

Interestingly, after the midday peak (approximately 3:07 PM), the larger-diameter (3 mm) systems began to outperform their smaller counterparts, particularly in terms of sustained efficiency under declining irradiance and stabilized thermal load. This behavior may be attributed to the greater flow volume and smoother oscillation stability in wider channels, which become more favorable once high-temperature transients subside. Furthermore, GO nanofluid proved superior to water in both diameter categories due to its higher thermal conductivity and improved wetting behavior, leading to more uniform heat extraction across the panel surface. These findings highlight that while smaller diameters excel under peak solar conditions due to stronger capillary effects, larger diameters offer thermal inertia benefits in later stages of the cycle, making hybrid nanofluid PHPs adaptable to varying real-world

solar profiles.

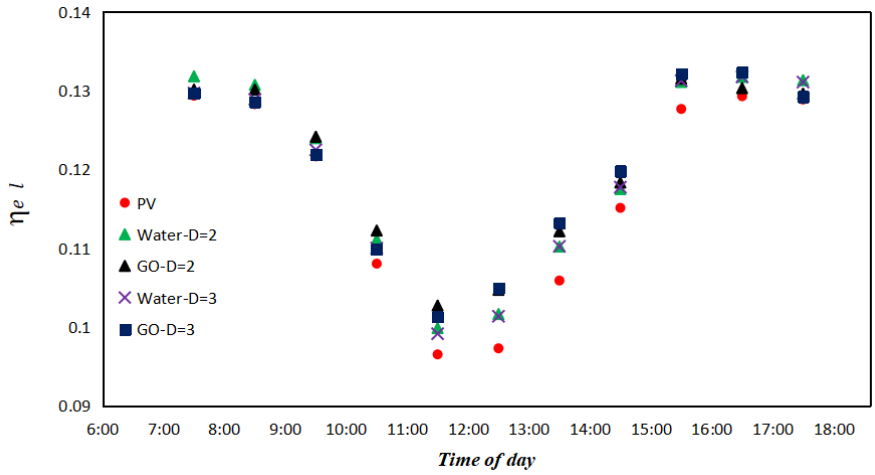

Figure 14. Effect of coolants on electrical efficiency.

Figure 15 illustrates the instantaneous thermal efficiency (η_{im}) of the PV system as a function of time for different working fluids (water and graphene oxide-based nanofluid) and inner diameters of the PHP. The data indicate that systems employing GO nanofluids consistently outperform those using water, regardless of PHP diameter. This improvement is primarily attributed to the superior thermophysical properties of GO nanofluids, including enhanced thermal conductivity and convective heat transfer, which facilitate more efficient heat removal from the PV surface.

Notably, during peak solar irradiance (around 12:00–13:00), the system with GO and D_i= 3 mm achieves the highest thermal efficiency, exceeding 8%. This suggests that a larger inner diameter enhances the circulation of the nanofluid within the PHP, thereby improving the overall thermal transport capability of the system under high thermal load conditions.

Conversely, the performance of water-cooled systems remains relatively lower throughout the day, with maximum efficiency observed to be below 4.5%, highlighting the limited thermal responsiveness of water under fluctuating heat flux.

These results emphasize the synergistic impact of nanofluid selection and geometric optimization of the PHP in maximizing PVT system efficiency, particularly during the critical midday period when thermal stress is highest.

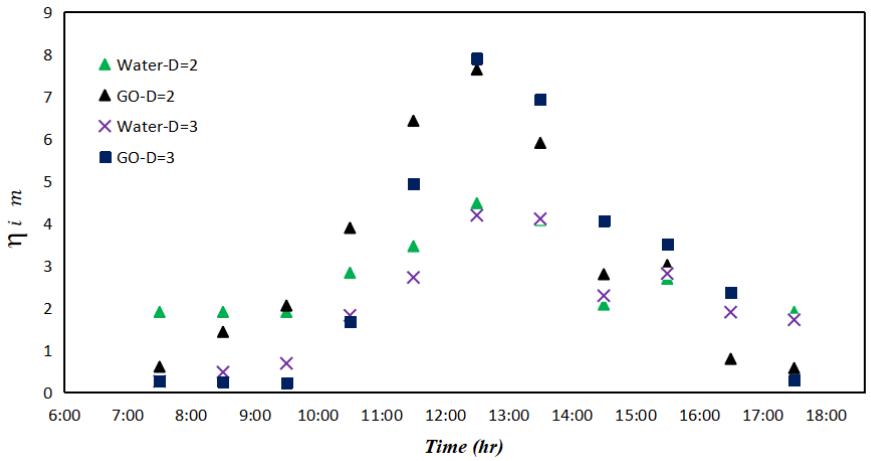

Figure 15. Enhancement of electrical efficiency using various cooling fluid.

3.3. Comparative Performance Analysis and Mechanistic Insight

The superior performance of the proposed 3D-PHP system can be attributed to the synergistic effect of geometrical design and coolant enhancement. Unlike 2D PHPs or conventional air/water-cooled systems, the 3D structure offers improved fluid motion due to additional oscillation pathways, enabling heat transfer in multiple directions and maintaining operation even under low-gravity or inclined conditions. Furthermore, the use of graphene oxide nanofluid significantly improves heat transfer through enhanced thermal conductivity (~ 6.8% over DI water) and lower surface tension, which facilitates earlier nucleation and more stable oscillations. Smaller internal diameters (2 mm) intensify capillary action, leading to lower startup temperatures and faster activation of oscillating motion. This capillarity-driven flow is especially crucial in passive cooling systems with no active pump. The experimental results demonstrated up to a 3.2% improvement in PV power output using the GO-based 2 mm PHP, outperforming traditional cooling methods that either suffer from high thermal resistance or freezing issues. Compared with previous work using standard heat pipes [21] and 2D configurations [23], the proposed design achieves lower thermal resistance (0.78 K/W vs. > 1.0 K/W) and higher electrical efficiency under the same irradiance levels. This confirms the advantages of integrating nanofluid-enhanced, geometrically optimized PHPs with PV panels for high-efficiency passive cooling.

4. Conclusions

This study demonstrates the effectiveness of a passive thermal management strategy for photovoltaic systems through the integration of a three-dimensional pulsating heat pipe (3D-PHP) charged with deionized water and graphene oxide (GO) nanofluid. Experimental results confirm that both the working fluid and the PHP inner diameter substantially influence thermal regulation and power output. Specifically, the system incorporating GO nanofluid and an optimized inner diameter achieved a peak power improvement exceeding 7.5% and reduced thermal resistance by over 30%, underscoring the critical role of nanofluid-enhanced heat transport.

The addition of sodium dodecyl sulfate (SDS) as a surfactant contributed to stabilizing PHP oscillations by modulating surface tension effects, while a copper plate interface efficiently transferred heat away from the PV module. These modifications enabled the system to maintain lower PV surface temperatures during peak irradiance without the need for external energy input.

The findings highlight the potential of 3D-PHPs with nanofluids as a scalable, low-cost, and energy-independent cooling solution for PV modules. However, the limited commercial application of PHP-integrated PV systems suggests a need for further research focused on system reliability, long-term performance, and integration with standard PV installations to bridge the gap toward practical deployment.

Although the current study demonstrates the efficiency of the 3D-PHP cooling system, future experimental designs should explore the influence of additional parameters such as inclination angle, long-term operational stability, and nanofluid concentration optimization. These will further validate the scalability and reliability of the system across different climates and operational contexts.

Author Contributions

Conceptualization, Investigation, Writing original draft, M.K.; Methodology, Validation, H.R.G.; Writing review & editing, P.G. All authors have read and agreed to the published version of the manuscript.

Funding

This work received no external funding.

Institutional Review Board Statement

Not applicable.

Informed Consent Statement

Not applicable.

Data Availability Statement

The data supporting the findings of this study are available from the corresponding author upon reasonable request.

Acknowledgments

The authors acknowledge Islamic Azad university Mashhad branch.

Conflicts of Interest

The authors declare no conflict of interest.

Abbreviation

A	**collector aperture area (m^2)**
C	heat capacity of flowing medium (J/kg k)
D	diameter
G	incident solar radiation (W /m^2)
I	electric current (A)
$\dot{m}$	mass flow rate
Q	heating power (W)
P	power (W)
T	temperature (°C)
R	thermal resistance (°C W^{-1})
V	voltage (V)
HP	Heat pipe
OHP	Oscillating heat pipe
PHP	Pulsating heat pipe
Pr	Prandtl number
PV	Photovoltaic
Re	Reynolds number
S	Speed
α	absorption ratio
β	packing factor
γ	specific heat ration
ρ	density
σ	surface tension
φ	volume fraction of the nanoparticles
η	efficiency
Subscripts	
a	ambient
air	air
c	condenser
el	electrical
e	evaporator
GO	graphene oxide
i	inner
im	Improvement
in	Input
mp	maximum power point
nf	nanofluid
oc	open-circuit

out	output
pv	Photovoltaic
rc	reference
s	solar collector
sc	short-circuit
w	wind

References

1. Kargaran, M. Enhanced Thermal Management of Photovoltaic Panels Using Super-Hydrophilic Oscillating Heat Pipes and Graphene Oxide Hybrid Nanofluid: Energy and Exergy Assessment. *Energy Convers. Manag.* **2025**, *27*, 101177.
2. Utomo, Bayu, Jo Darkwa, Dengfeng Du, and Mark Worall. Solar photovoltaic cooling and power enhancement systems: A review. *Renew. Sustain. Energy Rev.* 2025, *216*, 115644.
3. Bashirnezhad, K.; Kargaran, M.; Heris, S.Z.; et al. Improvement of Thermal, Energy and Exergy Performance of Flat Panel Solar Collector by Insertion of Perforated Strips and Hybrid CuO-MWCNTs Nanofluid. *Results Eng.* **2025**, *27*, 106120.
4. Kargaran, M.; Goshayeshi, H.R.; Azarberahman, S.; et al. Advanced Cooling of Photovoltaic Panels Using Hybrid Nanofluids Incorporating Graphene Oxide and Carbon Nanotubes. *Int. J. Energy Res.* **2025**, *2025*, 4345236.
5. Kargaran, M.; Goshayeshi, H.R.; Jajarm, A.R.A. A Novel Integrated Photovoltaic System with a Three-Dimensional Pulsating Heat Pipe. *Front. Heat Mass Transf.* **2024**, *22*, 1461–1476.
6. Ayadi, O.; Shadid, R.; Bani-Abdullah, A.; et al. Experimental Comparison Between Monocrystalline, Polycrystalline, and Thin-Film Solar Systems Under Sunny Climatic Conditions. *Energy Rep.* **2022**, *8*, 218–230.
7. Choubineh, N.; Jannesari, H.; Kasaeian, A. Experimental Study of the Effect of Using Phase Change Materials on the Performance of an Air-Cooled Photovoltaic System. *Renew. Sustain. Energy Rev.* **2019**, *101*, 103–111.
8. Schiro, F.; Benato, A.; Stoppato, A.; et al. Improving Photovoltaics Efficiency by Water Cooling: Modelling and Experimental Approach. *Energy* **2017**, *137*, 798–810.
9. Fu, H.D.; Pei, G.; Ji, J.; et al. Experimental Study of a Photovoltaic Solar-Assisted Heat-Pump/Heat-Pipe System. *Appl. Therm. Eng.* **2012**, *40*, 343–350.
10. Kazem, H.A.; Al-Waeli, A.A.; Chaichan, M.T.; et al. Enhancement of Photovoltaic Module Performance Using Passive Cooling (Fins): A Comprehensive Review. *Case Stud. Therm. Eng.* **2023**, *49*, 103316.
11. Chandel, S.S.; Agarwal, T. Review of Cooling Techniques Using Phase Change Materials for Enhancing Efficiency of Photovoltaic Power Systems. *Renew. Sustain. Energy Rev.* **2017**, *73*, 1342–1351.
12. Ali, H.M.; Shah, T.R.; Babar, H.; et al. Application of Nanofluids for Thermal Management of Photovoltaic Modules: A Review. In *Microfluidics and Nanofluidics*; Kandelousi, M.S., Ed.; IntechOpen: London, UK, 2018; pp. 35–59.
13. Alshukri, M.J.; Hussein, A.K.; Eidan, A.A.; et al. A Review on Applications and Techniques of Improving the Performance of Heat Pipe-Solar Collector Systems. *Sol. Energy* **2022**, *236*, 417–433.
14. Pagliarini, L.; Iwata, N.; Bozzoli, F. Pulsating Heat Pipes: Critical Review on Different Experimental Techniques. *Exp. Therm. Fluid Sci.* **2023**, *148*, 110980.
15. Ahmadian-Elmi, M.; Hajmohammadi, M.R.; Nourazar, S.S.; et al. Effect of Filling Ratio, Number of Loops, and Transverse Distance on the Performance of Pulsating Heat Pipe in a Microchannel Heat Sink. *Numer. Heat Transf. Part A Appl.* **2023**, *85*, 1278–1299.
16. Su, Z.; Hu, Y.; Zheng, S.; et al. Recent Advances in Visualization of Pulsating Heat Pipes: A Review. *Appl. Therm. Eng.* **2022**, *221*, 119867.
17. Alqahtani, A.A.; Edwardson, S.; Marengo, M.; et al. Performance of Flat-Plate, Flexible Polymeric Pulsating Heat Pipes at Different Bending Angles. *Appl. Therm. Eng.* **2022**, *216*, 118948.
18. Zhan, J.; Chen, X.; Ji, Y.; et al. Experimental Study of Ethane Pulsating Heat Pipe with Varying Evaporator Lengths Based on Pulse Tube Refrigerator. *Int. J. Refrig.* **2023**, *145*, 40–49.
19. Mameli, M.; Besagni, G.; Bansal, P.K.; et al. Innovations in Pulsating Heat Pipes: From Origins to Future Perspectives. *Appl. Therm. Eng.* **2022**, *203*, 117921.
20. Lin, Z.R.; Lee, Z.Y.; Zhang, L.W.; et al. An Experimental Study of Heat Transfer Characteristics in Miniature Loop Heat Pipes with Rectangular Shaped Evaporator. In Proceedings of the ASME 2011 Pacific Rim Technical Conference and Exhibition on Packaging and Integration of Electronic and Photonic Systems, Portland, OR,

USA, 6–8 July 2011.
21. Rittidech, S.; Donmaung, A.; Kumsombut, K. Experimental Study of the Performance of a Circular Tube Solar Collector with Closed-Loop Oscillating Heat-Pipe with Check Valve (CLOHP/CV). *Renew. Energy* **2009**, *34*, 2234–2238.
22. Kargarsharifabad, H.; Mamouri, S.J.; Shafii, M.B.; et al. Experimental Investigation of the Effect of Using Closed-Loop Pulsating Heat Pipe on the Performance of a Flat Plate Solar Collector. *J. Renew. Sustain. Energy* **2013**, *5*, 013106.
23. Patel, V.M.; Mehta, H.B. Influence of Working Fluids on Startup Mechanism and Thermal Performance of a Closed Loop Pulsating Heat Pipe. *Appl. Therm. Eng.* **2017**, *110*, 1568–1577.
24. Roslan, M.E.B.M.; Hassim, I. Solar PV System with Pulsating Heat Pipe Cooling. *Int. J. Electr. Eng. Comput. Sci.* **2019**, *14*, 311–318.
25. Wang, X.; Luo, L.; Xiang, J.; et al. A Comprehensive Review on the Application of Nanofluid in Heat Pipe Based on the Machine Learning: Theory, Application and Prediction. *Renew. Sustain. Energy Rev.* **2021**, *150*, 111434.
26. Ghorabaee, H.; Emami, M.R.S.; Moosakazemi, F.; et al. The Use of Nanofluids in Thermosyphon Heat Pipe: A Comprehensive Review. *Powder Technol.* **2021**, *394*, 250–269.
27. Dehaj, M.S.; Ahmadi, M.; Mohiabadi, M.Z. Assessment of a Heat Pipe Solar Collector with Nanofluids. *Environ. Sci. Pollut. Res.* **2021**, *28*, 5316–5331.
28. Allouhi, A.; Amine, M.B. Heat Pipe Flat Plate Solar Collectors Operating with Nanofluids. *Sol. Energy Mater. Sol. Cells* **2021**, *219*, 110798.
29. Nazari, M.A.; Ghasempour, R.; Ahmadi, M.H.; et al. Experimental Investigation of Graphene Oxide Nanofluid on Heat Transfer Enhancement of Pulsating Heat Pipe. *Int. Commun. Heat Mass Transf.* **2018**, *91*, 90–94.
30. Novoselov, K.S.; Blake, P.; Katsnelson, M.I. Graphene: Electronic Properties. *Encycl. Mater. Sci. Technol.* **2008**, *2008*, 1–6.
31. Kargaran, M.; Goshayeshi, H.R.; Saleh, S.R.; et al. Cooling Effect of 3D Oscillating Heat Pipe with Nanofluid on Photovoltaic Panel in Hot Climates. *Multiscale Multidiscip. Model. Exp. Des.* **2024**, *7*, 3215–3225.
32. Kargaran, M. Advanced Nanofluid-Assisted OHP–TEG Integration for Next-Generation Photovoltaic Thermal Management. *Energy* **2025**, 138024.
33. Thompson, S.M.; Cheng, P.; Ma, H.B. An Experimental Investigation of a Three-Dimensional Flat-Plate Oscillating Heat Pipe with Staggered Microchannels. *Int. J. Heat Mass Transf.* **2011**, *54*, 3951–3959.
34. Ling, Y.Z.; Zhang, X.S.; Wang, F.; et al. Performance Study of Phase Change Materials Coupled with Three-Dimensional Oscillating Heat Pipes with Different Structures for Electronic Cooling. *Renew. Energy* **2020**, *154*, 636–649.
35. Qu, J.; Zuo, A.; Liu, H.; et al. Three-Dimensional Oscillating Heat Pipes with Novel Structure for Latent Heat Thermal Energy Storage Application. *Appl. Therm. Eng.* **2021**, *187*, 116574.
36. Pagliarini, L.; Cattani, L.; Mameli, M.; et al. Global and Local Heat Transfer Behaviour of a Three-Dimensional Pulsating Heat Pipe: Combined Effect of the Heat Load, Orientation and Condenser Temperature. *Appl. Therm. Eng.* **2021**, *195*, 117144.
37. Jung, J.; Jeon, Y. Numerical Study on the Heat Transfer Characteristics of Three-Dimensional Pulsating Heat Pipe. *J. Mech. Sci. Technol.* **2023**, *37*, 4869–4876.
38. Dai, Y.; Zhang, R.; Qin, Z.; et al. Research on Heat Transfer Performance and Optimization of Three-Dimensional Array Pulsating Heat Pipe. *SSRN Electron.* **2023**, 1–33.
39. Zhang, D.; He, Z.; Guan, J.; et al. Heat Transfer and Flow Visualization of Pulsating Heat Pipe with Silica Nanofluid: An Experimental Study. *Int. J. Heat Mass Transf.* **2022**, *183*, 122100.
40. Jajarm, A.R.A.; Goshayeshi, H.R.; Bashirnezhad, K. Experimental Study of Thermal Performance of a Newly Designed Pulsating Heat Pipe with Fe_3O_4 Nanofluid-Exposed Magnetic Field and Corrugated Evaporator. *Int. J. Thermophys.* **2022**, *43*, 40.
41. Zhang, D.; He, Z.; Guan, J.; et al. Heat Transfer and Flow Visualization of Pulsating Heat Pipe with Silica Nanofluid: An Experimental Study. *Int. J. Heat Mass Transf.* **2022**, *183*, 122100.
42. Afsari, K.; Emami, M.R.S.; Zahmatkesh, S.; et al. Optimizing the Thermal Performance of the Thermosyphon Heat Pipe for Energy Saving with Graphene Oxide Nanofluid. *Energy* **2023**, *274*, 127422.
43. Chen, F.; Hu, M.; Badiei, A.; et al. Experimental and Numerical Investigation of a Novel Photovoltaic/Thermal System Using Micro-Channel Flat Loop Heat Pipe (PV/T-MCFLHP). *Int. J. Low-Carbon Technol.* **2020**, *15*, 513–527.
44. Agyekum, E.B.; PraveenKumar, S.; Alwan, N.T.; et al. Experimental Investigation of the Effect of a Combination of Active and Passive Cooling Mechanism on the Thermal Characteristics and Efficiency of Solar PV Module.

Inventions **2021**, *6(4)*, 63.
45. Zheng, Z.Z. Experimental Investigation on Surface Tension of Water-Based Graphene Oxide Nanofluids. *Adv. Mater. Res.* **2015**, *1082*, 297–301.
46. Zhang, Y.; Faghri, A. Advances and Unsolved Issues in Pulsating Heat Pipes. *Heat Transf. Eng.* **2008**, *29*, 20–44.
47. Santbergen, R.; Muthukumar, V.A.; Valckenborg, R.M.E.; et al. Calculation of Irradiance Distribution on PV Modules by Combining Sky and Sensitivity Maps. *Sol. Energy* **2017**, *150*, 49–54.
48. Hassan, A.; Abbas, S.; Yousuf, S.; et al. An Experimental and Numerical Study on the Impact of Various Parameters in Improving the Heat Transfer Performance Characteristics of a Water Based Photovoltaic Thermal System. *Renew. Energy* **2023**, *202*, 499–512.
49. Fouad, M.M.; Shihata, L.A.; Morgan, E.I. An Integrated Review of Factors Influencing the Performance of Photovoltaic Panels. *Renew. Sustain. Energy Rev.* **2017**, *80*, 1499–1511.
50. Kargaran, M.; Goshayeshi, H.R.; Saleh, S.R.; et al. Novel Cooling System for Free-Standing Photovoltaic Panels. *Energy Sources Part A Recov. Util. Environ. Eff.* **2024**, *46*, 8155–8170.